

Effects of Tall Fescue Biochar on the Adsorption Behavior of Desethyl-Atrazine in Different Types of Soil

Wanting Li,^a Ruifeng Shan,^{a,b,*} Yuna Fan,^a and Xiaoyin Sun^{a,b}

Desethyl-atrazine (DEA) is a metabolite of atrazine that exerts a considerable influence on the environment. In this study, tall fescue biochar was prepared by pyrolysis at 500 °C, and batch experiments were conducted to explore its effect on the adsorption behavior of DEA in red soil, brown soil, and black soil. The addition of biochar increased the equilibrium amount of DEA adsorption for the three soil types. A pseudo-second-order kinetic model most closely fit the DEA adsorption kinetics of the three soils with and without biochar, with a determination coefficient (R^2) of 0.962 to 0.999. The isothermal DEA adsorption process of soils with and without biochar was optimally described by the Freundlich and Langmuir isothermal adsorption models with R^2 values of 0.98 and above. The DEA adsorption process in the pristine soil involved an exothermic reaction, which became an endothermic reaction after the addition of biochar. Partitioning was dominant throughout the entire DEA adsorption process of the three pristine soils. Conversely, in soils with biochar, surface adsorption represented a greater contribution toward DEA adsorption under conditions of low equilibrium concentration. The overall results revealed that the tall fescue biochar was an effective adsorbent for DEA polluted soil.

Keywords: Tall fescue biochar; Desethyl-atrazine; Surface adsorption; Partitioning

Contact information: a: Key Laboratory of Nansihu Lake Wetland Ecological Conservation & Environmental Protection (Shandong Province), College of Geography and Tourism, Qufu Normal University, Rizhao 276826, People's Republic of China; b: Rizhao Key Laboratory of Territory Spatial Planning and Ecological Construction, Rizhao 276826, People's Republic of China;

* Corresponding author: ruiheng_shan@163.com

INTRODUCTION

In the last 30 years, China has become one of the top users and producers of pesticides in the world (Grung *et al.* 2015). Most pesticides have relatively high polarity and strong persistence and degrade to form complex metabolites in the environment (Montiel-Leon *et al.* 2019b). For example, in the Jucar River in Spain, some metabolites have been detected more frequently and at higher levels than parent compounds such as atrazine and terbumeton (Aguilar *et al.* 2017). Therefore, the presence of pesticide metabolites in the environment is of great concern. Desethyl-atrazine (DEA) is a metabolite formed by the physicochemical process and microbial degradation of its parent atrazine in soil, which is widely distributed in environmental media (Guo *et al.* 2016; Yu *et al.* 2018). Groundwater research in Iowa (USA) reported a DEA detection frequency of 32.1%, ranked only second to its parent compound atrazine (37.4%) and higher than deisopropylatrazine (DIA) (21.4%) and hydroxyatrazine (HA) (11.4%) (Kolpin *et al.* 2000). Montiel-Leon *et al.* (2019a) studied the spatial distribution of pesticides in the St. Lawrence River and its tributaries in Quebec, Canada and reported a DEA detection

frequency of 47%, which was only lower than that of glyphosate (84%), atrazine (82%), and thiamethoxam (59%). Moreover, atrazine (75%) and DEA (60.6%) presented the highest detection frequency in rural surface water and groundwater in Henan Province, China (Yu *et al.* 2018).

Toxicological studies have shown that DEA has similar toxicity to its parent compound atrazine (Kumar and Singh 2016). Sánchez *et al.* (2020) found that atrazine in soil pore water predominantly exists in the form of DEA and DIA, which accounted for 59% of the total amount of residual atrazine after a 19-day experiment, indicating that DEA has relatively high water solubility, strong polarity, and high stability. Moreover, the DEA content in the parts of plants that were above the ground was much higher than that in the parts of the root, thereby posing a potential threat to human health. Despite atrazine being listed as a prohibited pesticide by the European Commission (2009), atrazine and its metabolite DEA are still currently present in the Jucar river (Aguilar *et al.* 2017). This may reflect the fact that atrazine and DEA accumulate slowly in the field and eventually flow into river systems (Masia *et al.* 2013), suggesting that DEA can exist in environmental media for a long time and lead to the risk of extensive pollution. Therefore, it is necessary to explore low-cost and environmentally friendly remediation methods.

Previously, the degradation of atrazine and its major metabolites (DEA and DIA) in water by photocatalytic oxidation under sunlight has achieved good results (Komtchou *et al.* 2018). The use of a carbon source plus zero-valent iron under aerobic conditions can also effectively promote the dissipation of atrazine and DEA at a relatively low pollution level (Kerminen *et al.* 2017). However, different remediation methods vary considerably and are limited by high energy consumption and excessive pollutant concentrations. Biochar has a developed porous structure and a large specific area, rendering it a good adsorbent for a variety of organic and inorganic pollutants; it is produced *via* the pyrolysis of waste biomass materials under anoxic conditions (Sun *et al.* 2017; Chen *et al.* 2020). In addition, biochar is rich in carbon, which is conducive to the fixation of carbon in the environment, thereby decreasing greenhouse gas emissions and mitigating global warming (Ding *et al.* 2019).

The method of adsorbing pesticide residues from environmental media using biochar has attracted increasing attention. For example, Wei *et al.* (2017) suggested that the addition of rice husk biochar to soil had a significant adsorption effect on the herbicide alachlor, with its adsorption capacity being related to the physicochemical properties of biochar, such as pore structure and surface functional groups. Okoya *et al.* (2020) compared the adsorption effect of activated carbon and rice husk biochar on chlorpyrifos, which decreased the chlorpyrifos content in soil by 93.7% and 94.5%, respectively. Therefore, rice husk biochar had a more significant adsorption effect on chlorpyrifos and could be used as a substitute adsorbent for activated carbon. Binh and Kajitvichyanukul (2019) suggested that coconut silk biochar exhibited a strong adsorption effect on dichlorvos, with the maximum adsorption amount of the Langmuir model fitting a parameter reaching 90.9 mg·g⁻¹. However, these studies typically concentrated on the adsorption of pesticides for a single type of soil, with few studies investigating the adsorption behavior of pesticides for various types of soil. The physicochemical properties of soil determine the fate of pollutants in the environment, as well as the feasibility of the remediation technology of contaminated soil (Ahmed *et al.* 2018). Therefore, as the physicochemical properties of soil are important factors affecting the environmental behavior of pesticides in the soil-biochar system, it is necessary to study the adsorption behavior of pesticides for different types of soil.

Red soil, brown soil, and black soil exhibit different physicochemical properties such as pH values, cation exchange capacity, organic matter content, nutrient element content, and soil particle size, leading to diverse pesticide adsorption behaviors. Zhang *et al.* (2018a) found that the adsorption behavior of imidacloprid, clothianidin, and thiamethoxam in four agricultural soils was predominantly influenced by the soil organic matter content. Moreover, Hall *et al.* (2015) investigated the adsorption behaviors and leaching risks of six herbicides in three tropical soils in Hawaii; they suggested that pesticide adsorption was determined by local soil properties, whereas leaching risks could be predicted by soil property parameters. Therefore, pesticide adsorption behavior should be evaluated in different types of soils to predict their fate and ecological risk in environmental media.

Most previous studies have focused on the adsorption of the parent pesticide compound by the biochar-soil system; however, few studies have investigated the adsorption process of pesticide metabolites by biochar. This study introduces a novel biochar material derived from tall fescue, which is widely used for family gardens, golf lawns, and urban landscapes, and prepared by pyrolysis at 500 °C. The main purpose of the study is to explore the effect of tall fescue biochar on DEA adsorption from red soil, brown soil, and black soil and investigate the main mechanism of adsorption.

EXPERIMENTAL

Sample Preparation and Treatment

Red, brown, and black surface soil (0 to 10 cm) was sampled from the Jiangxi, Shandong, and Jilin provinces in China, respectively. After sampling, the soil was dried, homogenized, and screened to remove plant tissue. The basic physicochemical properties of the three types of soil are described in the authors' previous study (Li *et al.* 2020). The organic matter content decreased in the following order: black soil > brown soil > red soil. Except for the alkaline black soil, with a pH of 7.86, the red soil (pH = 6.29) and brown soil (pH = 4.70) were acidic. The red soil was predominantly clay, accounting for 37.8%. Sand (46.0%) and silt (39.51%), which accounted for the largest proportion of brown and black soil, respectively. The DEA standard solution with purity of 99.9% was purchased from Dr. Ehrenstorfer trading company (Augsburg, Germany). The DEA solution was dissolved in methanol to prepare a 100 mg·L⁻¹ stock solution, which was stored at 4 °C.

Preparation and Characterization of Tall Fescue Biochar

The tall fescue was sampled from Rizhao, Shandong province, China, then cleaned with tap water, dried to constant weight at 50 °C, and ground through an 18-mesh sieve. The tall fescue material was pyrolyzed under an N₂ atmosphere in a muffle furnace. The material was heated at 15 °C·min⁻¹ until the pyrolysis temperature reached 500 °C. It was then continuously heated for 2 h and cooled to room temperature. The tall fescue biochar was ground, sifted through 80-mesh screens, and sealed in a dry container for subsequent analysis. The characterization of tall fescue biochar methods were shown in the authors' previous study (Li *et al.* 2020). Briefly, the surface structure of the biochar was analyzed by a scanning electron microscope (SEM, QUANTA Q400, USA). The specific surface area and pore structure of tall fescue biochar was measured by the Brunauer-Emmett-Teller (BET) method. The element composition of the biochar was analyzed by a Vario macro cube elemental analyzer (Vario macro cube, Germany). The surface functional groups was

detected by Fourier transform infrared (FTIR) spectroscopy (4000-400 cm^{-1} wavenumbers, IRTracer-100, Shimadzu, Japan). The pH value of the biochar was measured by pH meter (PHS-3C, Shanghai, China).

Adsorption Experiment

A batch experiment was used to explore the DEA adsorption behavior of the three types of soil. Two grams of each soil were placed in a 50-mL Teflon centrifuge tube for an isothermal adsorption experiment, with 0.1 g of tall fescue biochar added to the biochar treatment group (BC soil). Then, 0.01 $\text{mol}\cdot\text{L}^{-1}$ of CaCl_2 and 200 $\text{mg}\cdot\text{L}^{-1}$ of NaN_3 was added to the reaction system to enhance the ionic strength and inhibit the microbial degradation of analyte, respectively. After 2 h of pre-equilibrium, 10 mL of DEA stock solution was diluted to obtain initial concentrations of 0.5, 1, 5, 10, and 20 $\mu\text{g}\cdot\text{mL}^{-1}$. The centrifuge tubes were covered tightly using lids, shaken thoroughly, and placed in a thermostatic oscillator covered with aluminum foil. The centrifuge tubes were oscillated for 24 h at 200 rpm and 25 °C, after which the samples were extracted to determine the equilibrium concentration of DEA. A kinetic pre-experiment showed that DEA adsorption in the three types of soil with and without biochar entered in an equilibrium adsorption stage prior to 24 h, with the concentration of DEA in the solution approximately unchanged. On this basis, two temperature gradients (15 and 35 °C) were employed for the adsorption thermodynamics experiment. In the adsorption kinetics experiment, the initial concentration of DEA was set at 5 $\text{mg}\cdot\text{L}^{-1}$ and the centrifuge tubes were oscillated at 200 rpm and 25 °C. The samples were extracted after 35 min, 180 min (3 h), 360 min (6 h), 540 min (9 h), 1,290 min (21.5 h), 1,440 min (24 h), and 2,880 min (48 h) of oscillation.

Three replicates of each experiment group were performed. The oscillating samples taken from the three experiments (adsorption kinetics, adsorption isotherm, and adsorption thermodynamics) were left to stand for 10 min. Gravity was used to separate the solution from the biochar and soil solids in the mixed system. The supernatant was filtered through a 0.22- μm membrane and centrifuged at 4,000 rpm for 10 min. Then, the supernatant was filtered through a 0.45- μm membrane, and the equilibrium concentration of DEA ($\mu\text{g}\cdot\text{mL}^{-1}$) was determined by high performance liquid chromatography (HPLC) (1260II, Agilent Technologies Inc., Santa Clara, CA, USA) with a Gemini C18 chromatographic column (150 \times 4.6 mm; 4 μm). The flowing phase contained methanol, and water (1:7 v/v) moved at a rate of 0.8 $\text{mL}\cdot\text{min}^{-1}$. The photo diode array (PDA) detector operated at a wavelength of 220 nm, and the injection volume was 10 μL . The column temperature was set to 35 °C. Three parallels of DEA standard solution were added to the blank groups to determine the recovery rate. The recovery rate of DEA was 95 to 105%. The external standard method was used as a quality control. Seven concentration gradients of DEA standard solution were prepared prior to injection. The correlation coefficient (R^2) between the actual concentration of the DEA standard solution and the peak area was greater than 0.995.

Data Analysis

All data were analyzed by using origin 8.0 software (OriginLab, Northampton, MA, USA). The adsorption amount of DEA was calculated using Eq. 1,

$$q = \frac{(C_e - C_0) \cdot V}{m} \quad (1)$$

where q ($\mu\text{g}\cdot\text{g}^{-1}$) is the DEA adsorption amount for the three types of soil, C_0 ($\mu\text{g}\cdot\text{mL}^{-1}$) is the initial concentration of DEA, C_e ($\mu\text{g}\cdot\text{mL}^{-1}$) is the DEA equilibrium concentration, V (mL) is the volume of the solution, and m (g) is the mass of soil.

A pseudo second-order kinetic model (Eq. 2), Elovich model (Eq. 3), pseudo first-order kinetic model (Eq. 4), and intra-particle diffusion model (Eq. 5) were used to describe the adsorption kinetic data as follows,

$$\frac{t}{q_t} = \frac{1}{k_2 q_e^2} + \frac{t}{q_e} \quad (2)$$

$$q_t = A + B \cdot \ln t \quad (3)$$

$$q_t = q_e (1 - e^{-k_1 t}) \quad (4)$$

$$q_t = k_p \cdot t^{\frac{1}{2}} + C \quad (5)$$

where q_t ($\mu\text{g}\cdot\text{g}^{-1}$) is the DEA adsorption amount of three types of soil with and without biochar at time t (min), q_e ($\mu\text{g}\cdot\text{g}^{-1}$) is the equilibrium DEA adsorption amount, k_2 ($\text{mg}\cdot\mu\text{g}^{-1}\cdot\text{min}^{-1}$), k_1 ($\text{mg}\cdot\mu\text{g}^{-1}\cdot\text{min}^{-1}$), and k_p ($\mu\text{g}\cdot\text{mg}^{-1}\cdot\text{min}^{-1/2}$) are the pseudo second-order kinetic, pseudo first-order kinetic, and intra-particle diffusion constant, respectively, A is a constant related to the initial concentration, B is the adsorption activation energy constant, and C is a parameter which represents the effect of boundary layers.

The Freundlich (Eq. 6) and Langmuir (Eq. 7) models were used to describe the adsorption isotherm,

$$\ln q_e = \ln K_f + \ln C_e \cdot 1/n \quad (6)$$

$$\frac{1}{q_e} = \frac{1}{q_{\max}} + \frac{1}{K_L q_{\max} C_e} \quad (7)$$

where K_f [$(\mu\text{g}\cdot\text{mg}^{-1})/(\mu\text{g}\cdot\text{mL}^{-1})^n$] is Freundlich's coefficient, q_{\max} ($\mu\text{g}\cdot\text{g}^{-1}$) is the maximal DEA adsorption amount of the three soils with and without biochar, $1/n$ reveals the nonlinear degree of the adsorption isotherm, distinct adsorption mechanism, and adsorption intensity, K_L is a parameter of the Langmuir model that demonstrates the bond energy of the adsorbent surface, and C_e and q_e are defined in Eqs. 1 and 2, respectively.

The Gibbs free energy (ΔG , in $\text{kJ}\cdot\text{mol}^{-1}$) was used to describe the thermodynamic pattern and energy changes of the adsorption process following Eqs. 7 and 8,

$$\Delta G = -RT \ln K_f \quad (8)$$

$$\Delta G = \Delta H - T\Delta S \quad (9)$$

where R [$\text{J}\cdot(\text{mol}\cdot\text{K})^{-1}$] is the molar gas constant with a value of 8.314, T (K) is the absolute temperature, and K_f is the value of Freundlich's coefficient Eq. 6. The enthalpy change (ΔH , in $\text{kJ}\cdot\text{mol}^{-1}$) indicates transformation of the reaction system conditions, and ΔS ($\text{kJ}\cdot\text{mol}^{-1}\cdot\text{K}^{-1}$) represents a change of the disorder degree in a system.

The adsorption behavior of DEA in pristine soil and BC soil was divided into two parts: surface adsorption and partitioning. To explore the adsorption mechanism of DEA in soil and BC soil, Eqs. 10 through 13 were used to quantify the relative contribution of DEA partitioning and surface adsorption for the three types of soil and BC soil (Zhao *et al.* 2019),

$$Q_T = Q_P + Q_A \quad (10)$$

where Q_T represents the total DEA adsorption amount for the three soils and BC soils, and Q_P and Q_A represent the adsorption amount related to partitioning and surface adsorption, respectively. According to the characteristics of partitioning and surface adsorption, the organic pollutant is adsorbed by the surface-active adsorption sites of soil and biochar at relatively low concentrations. However, with increased pollutant concentration, the surface adsorption sites of soil and biochar become completely occupied and saturated; then, partitioning plays a dominant role in the adsorption process (Wang *et al.* 2019). Therefore, the adsorption contribution equation was converted to,

$$Q_T = Q_P + Q_A = KC_e + Q_A \quad (11)$$

where K is the partitioning coefficient, which is the slope obtained by linear fitting of the adsorption isotherm in a relatively high concentration range of $C_e / S_w > 0.2$ (ratio of equilibrium concentration to aqueous solubility). Therefore, the contribution of partitioning and surface adsorption to the total adsorption amount can be expressed by Eqs. 12 and 13, respectively:

$$Q_P = KC_e \quad (12)$$

$$Q_A = Q_T - KC_e \quad (13)$$

RESULTS AND DISCUSSION

Effects of Biochar on DEA Adsorption Kinetics in Different Soil Types

The DEA adsorption kinetics differed between the three pristine soils and BC soils (Fig. 1). However, the DEA adsorption process was similar for the three soils and BC soils and involved three stages: fast, slow, and equilibrium. During the first 180 min of the adsorption process, the slopes of the adsorption curves were relatively steep, and the DEA adsorption rate was relatively high in both pristine and BC soil. The DEA adsorption amount of red soil, brown soil, and black soil reached 69.3%, 74.4%, and 98.2% of the equilibrium adsorption amount within the first 180 min, respectively. The adsorption amount of BC soil accounted for 39.9 to 50.8% of the equilibrium DEA adsorption amount within the first 180 min, which was remarkable less than that for pristine soil. This indicates that DEA adsorption occurred primarily in the slow adsorption stage (after 180 min) in BC soil, but during the fast adsorption stage in the pristine soil without biochar addition. This may be because the biochar has a developed pore structure and huge specific surface area. In comparison with the pristine soil, biochar contains denser adsorption domains and active adsorption sites on its surface (Li *et al.* 2020), whereas the active adsorption sites on the surface of pristine soil become gradually saturated after 180 min of the adsorption process. However, a large number of unoccupied low-energy active adsorption sites remain on the surface of BC soil due to the application of biochar; these can be used for DEA adsorption in the slow adsorption stage.

In addition, the equilibrium DEA adsorption amount of BC soil in the equilibrium state was greater than that of pristine soil. Therefore, the ratio of DEA adsorption within the first 180 min to the equilibrium adsorption amount was higher for pristine soil than BC soil. During 180 to 1440 min, the DEA adsorption rate of soil and BC soil slowed down, which illustrates that the adsorption process entered the slow stage. This was mainly because the DEA molecule was rapidly adsorbed by active adsorption sites on the surface

of the soil and BC soil during the initial stage of the reaction (Uwamungu *et al.* 2019). As the reaction progressed, active adsorption sites were gradually occupied by DEA, which then entered the micropore structure inside the biochar and soil for relatively slow micropore filling. The DEA adsorption rate of the three soils and BC soils gradually slowed down and finally reached the equilibrium adsorption stage. In addition, the concentration gradient between soil / BC soil and DEA solution in the slow adsorption stage was smaller than that in the fast adsorption stage. Therefore, the reaction rate slowed down. The adsorption reaction system reached the equilibrium stage after 1440 min, at which point the DEA concentration in the equilibrium solution was approximately unchanged. The actual equilibrium DEA adsorption amounts of red soil, brown soil, black soil, BC red soil, BC brown soil, and BC black soil were 1.27, 1.97, 3.24, 19.39, 14.16, and 15.68 $\text{mg}\cdot\text{kg}^{-1}$, respectively. The equilibrium adsorption amounts were ranked as follows: BC red soil > BC black soil > BC brown soil > black soil > brown soil > red soil. The difference of adsorption capacity between pristine soil and BC soil for DEA was partly attributed to the difference of surface micropore structure between them. Based on the authors' previous study (Li *et al.* 2020), the SEM analysis demonstrated a developed pore structure and a clear reticulation formation of the tall fescue biochar. Therefore, the DEA molecule filled into the micropores on the surface of soils and BC soils may be a main mechanism during the adsorption reaction. Hence, on the basis of micropore regulation theory, which proposed by Braida *et al.* (2003), the adsorption reaction tended to be equilibrium may have been due to the DEA having entered and expanded the micropores of the biochar and soil, and thermodynamic changes having deformed the surrounding micropores. The DEA adsorbed in the deformed micropores was more difficult to desorb; thus, dynamic equilibrium between adsorption and desorption was finally achieved.

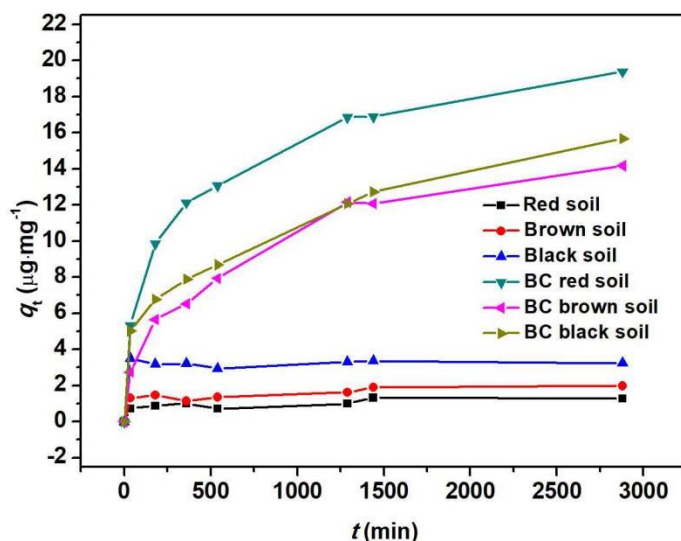


Fig. 1. DEA adsorption kinetic curves of three pristine soils and three BC soils

As shown in Fig. 1, the DEA adsorption amount of all three soils increased after adding biochar, which was consistent with the results of Wang *et al.* (2019). This may also be because of the large number of active DEA adsorption sites in the biochar, which enhance surface adsorption and pore filling of DEA in the biochar-soil system, thereby increasing the DEA adsorption capacity of soil. Due to the abundant surface functional

groups and high degree of aromatization of the tall fescue biochar (Li *et al.* 2020), the aromatic functional groups of biochar can be used as electron donors or acceptors to trigger electron donor–receptor (EDA) reactions with aromatic compounds, which improves the adsorption of DEA. Zhang *et al.* (2013) suggested that biochar exerted an obvious adsorption effect on most pesticides with an aromatic ring structure, such as simazine and atrazine. In addition, biochar presents strong affinity with most pesticides due to its hydrophobicity (Qiu *et al.* 2009). The actual equilibrium adsorption amounts of DEA in BC red soil, BC brown soil, and BC black soil were 19.4, 14.2, and 15.7 mg·kg⁻¹, respectively, *i.e.*, BC red soil > BC brown soil > BC black soil. In comparison to the pristine soil, the DEA adsorption amount increased 1427%, 619%, and 385% for BC red soil, BC brown soil, and BC black soil, respectively. This suggests that the remediation effect of biochar on the adsorption capacity of the three soils decreased in the following order: red soil > brown soil > black soil. This contrasts with the relative organic matter content of the three soils (Li *et al.* 2020), which may be because the soil organic matter competes for the adsorption sites on the surface of the biochar or blocks the pores of the biochar (Zhang *et al.* 2020), leading to a decrease in the DEA adsorption capacity of biochar. Therefore, the remediation effect of biochar on the soil adsorption capacity is affected by the physicochemical properties of the soil, among which the organic matter content plays an important role.

The pseudo-second-order kinetic model (Eq. 2), Elovich model (Eq. 3), and pseudo first-order kinetic model (Eq. 4) were used to fit the adsorption data of the three soils and BC soils for DEA, and the fitting parameters are shown in Table 1.

Table 1. DEA Adsorption Kinetic Fitting Parameters for the Three Soils and BC Soils

Soil	Pseudo Second-order			Elovich			Pseudo First-order		
	q_e ($\mu\text{g/g}$)	k_2 [$\mu\text{g}/(\text{m g}\cdot\text{min})$]	R^2	A	B	R^2	q_e ($\mu\text{g/g}$)	k_1 [$\mu\text{g}/(\text{mg}\cdot\text{min})$]	R^2
Red soil	1.292	0.0060	0.964 ^{**}	0.236	0.122	0.488 ^{**}	1.000	0.878	0.665 ^{**}
Brown soil	1.986	0.0050	0.985 ^{**}	0.497	0.145	0.311 ^{**}	1.537	7.792*10 ¹¹	0.749 ^{**}
Black soil	3.266	0.0750	0.999 ^{**}	3.449	0.032	0.104 ^{**}	3.250	1.286*10 ¹³	0.979 ^{**}
BC red soil	19.841	0.0003	0.988 ^{**}	6.593	3.223	0.992 ^{**}	13.359	1.316*10 ¹³	0.450 ^{**}
BC brown soil	15.000	0.0002	0.969 ^{**}	8.003	2.707	0.933 ^{**}	8.749	4.266*10 ¹²	0.292 ^{**}
BC black soil	16.015	0.0002	0.962 ^{**}	4.995	2.400	0.877 ^{**}	9.835	1.320*10 ¹³	0.415 ^{**}

According to the correlation coefficient (R^2) fitted by the three kinetic models, the pseudo-second-order kinetic model can optimally describe the adsorption kinetic process of DEA in all soils, with R^2 values as high as 0.962 to 0.999, which were higher than those of the Elovich model (0.104 to 0.992) and pseudo first-order kinetic model (0.292 to 0.979). These kinetic models all had extremely significant correlations ($P < 0.01$). The difference between the theoretical equilibrium adsorption amount ($q_{e, cal}$) calculated by the pseudo second-order kinetic model and the actual equilibrium adsorption amount ($q_{e, exp}$) was only 2.3%. This indicates that the rate of the adsorption process of these soils for DEA was limited by diffusion effects (Hubbe *et al.* 2019).

To investigate the rate-limiting factors involved in the DEA adsorption process of the soil-biochar system, the adsorption kinetic data were analyzed using the intra-particle diffusion model (Eq. 5), as shown in Fig. 2. Intraparticle diffusion was a factor of rate limiting in the adsorption process if a plot of adsorption amount against the square root of the contact time performed a straight line (Pholosi *et al.* 2020). The fitting linear plot of q_t versus $t^{1/2}$ of three BC soils was linear but did not pass through the origin of coordinates, namely $C \neq 0$, which indicated that the rate-limiting factor of the DEA adsorption process for BC soils was not only intra-particle diffusion, but also boundary layer diffusion (Wang and Zhang 2021). The C values of the intraparticle diffusion model were ranked as follows: BC red soil > BC black soil > BC brown soil, which illustrated that the boundary layer effect increased in sequence. The kinetic experimental data of three soils without biochar manifested a less obvious linear relationship between q_t and $t^{1/2}$ than the BC soils (R^2 value of -0.1928 to 0.6814).

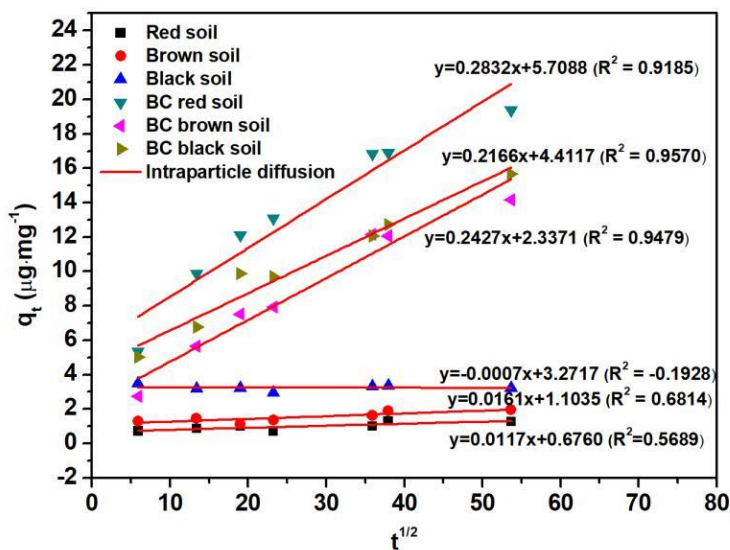


Fig. 2. Fitting curves of the intra-particle diffusion model for DEA in three soils and BC soils

Effects of Biochar on DEA Adsorption Isotherms

The DEA adsorption isotherms of three types of soil and BC soil are shown in Fig. 3. The DEA adsorption amount increased with increasing DEA concentration in the equilibrium solution. This may be attributed to an increase of DEA molecules near the biochar, which increased the mass transfer power and DEA adsorption capacity of the soils (Aljeboree *et al.* 2015). The DEA adsorption isotherms of the pristine soil were

approximately linear, whereas the DEA adsorption isotherms for the three BC soils were concave to the equilibrium concentration axis and exhibited a nonlinear growth trend. Dehydration and dehydrogenation of biochar during the pyrolysis process resulted in the formation of biochar surface pores, which provided a large number of adsorption sites and somewhat determined the DEA adsorption capacity of biochar. The adsorption isotherm curve of DEA for BC soil showed a rapid upward trend and a relatively steep slope when the equilibrium concentration was low. During this process, DEA molecules were adsorbed by high-energy active adsorption sites on the surface of the biochar. With an increase of DEA concentration in the equilibrium solution, the upward trend of the isotherms gradually slowed down and the slope of the curve decreased. During this process, the high-energy active adsorption sites on the biochar surface were occupied, and DEA molecules were adsorbed by the low-energy active adsorption sites, which led to a reduction in the adsorption rate. In addition, the pesticide adsorption capacity of biochar may depend on the hydrogen bond that forms between pesticide and oxygen-containing functional groups on the biochar surface (Wang *et al.* 2011). When the equilibrium concentration of DEA increased, the amount of electrons supplied by oxygen-containing functional groups on the surface of the biochar gradually decreased, thus decreasing the amount of DEA adsorption.

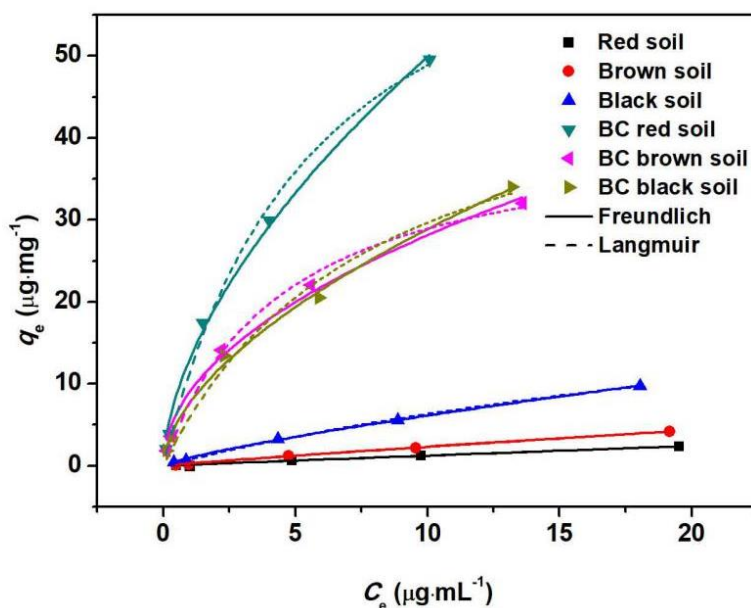


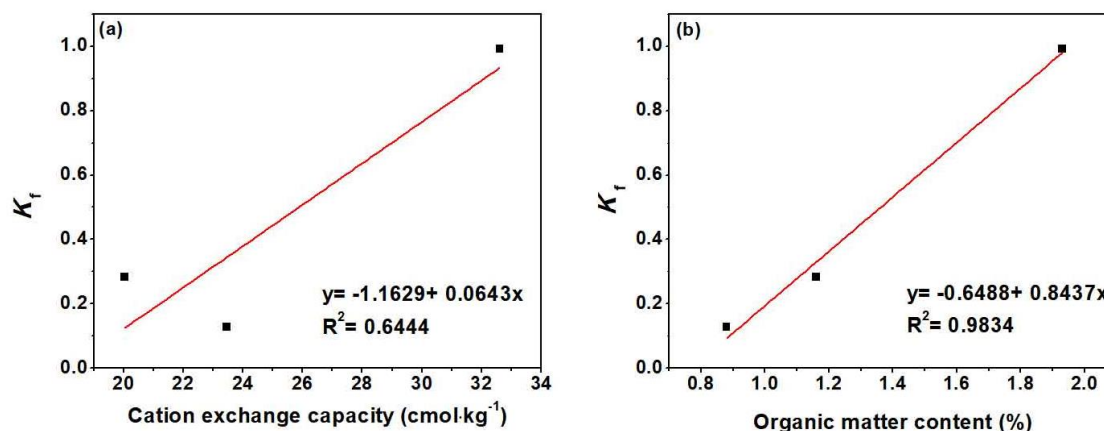
Fig. 3. DEA adsorption isotherms for the three soils and three BC soils

The Langmuir and Freundlich models were used to fit the isothermal adsorption results of pristine soils and BC soils (Table 2). According to Table 2, the Freundlich model well described the DEA adsorption data for all soils, with R^2 values of 0.988 to 0.999. Excellent fits also were obtained with the Langmuir model (R^2 0.979 to 0.999). Figure 3 also shows the fits of the Freundlich and Langmuir isotherms. To within the error of replication of the experimental data, the DEA adsorption behavior of pristine and BC soils were consistent with both models. The results were similar to those of Wang *et al.* (2019), who found better agreement with the Freundlich isotherm. After adding biochar to the soil, the soil still occupies a major portion of the biochar-soil system; therefore, adsorption on a heterogeneous surface was still dominant in the adsorption process (Bogusz *et al.* 2017).

Table 2. DEA Adsorption Isotherm Parameters for Three Soils and BC Soils

Soil	Freundlich			Langmuir		
	K_f	$1/n$	R^2	K_L	q_{max} (mg/kg)	R^2
Red Soil	0.128	0.982	0.988**	0.0039	33.169	0.989**
Brown Soil	0.283	0.911	0.998**	0.0092	27.644	0.999**
Black Soil	0.992	0.791	0.999**	0.0275	29.297	0.998**
BC Red Soil	13.005	0.584	0.995**	0.175	76.829	0.994**
BC Brown Soil	9.013	0.494	0.989**	0.223	41.918	0.992**
BC Black Soil	7.667	0.576	0.996**	0.125	53.415	0.979**

The adsorption constant, K_f value, of the Freundlich model is related to the bonding energy between adsorbent and adsorbate (Asadullah *et al.* 2019). The K_f value demonstrated the relative sorption affinity and sorption energy of the soils for DEA (Wei *et al.* 2017). Therefore, the adsorption affinity between soil and DEA molecule increases with increasing K_f value. The K_f value increased after adding biochar to the soil (Table 2), which demonstrated that the application of tall fescue biochar increased the adsorption affinity between the soil and DEA. Due to the different physicochemical properties of the soil, the three pristine soils exhibited different adsorption affinity for DEA, with K_f values decreasing in the following order: black soil > brown soil > red soil. The organic matter content of the three pristine soils decreases in the same order (Li *et al.* 2020). Figure 4a and b presents positive correlations between the soil cation exchange capacity (CEC), organic matter (OM) content, and adsorption constant K_f .

**Fig. 4.** Correlation of the Freundlich fitting parameter K_f value with (a) soil cation exchange capacity and (b) soil organic matter content

A greater correlation was observed between K_f and soil OM content ($R^2 = 0.9834$) than CEC ($R^2 = 0.6444$). This may be because the soil CEC is typically related to the OM content (Zhang *et al.* 2020). Thus, the adsorption affinity between the three pristine soils and DEA increased with increasing soil CEC and OM content, as also reported by Zhang *et al.* (2020), which may reflect the presence of carboxyl, phenolic hydroxyl, alcohol hydroxyl, quinone, hydroxyquinone, and lactone functional groups in soil OM. These functional groups enhance the adsorption affinity of soil OM for pesticide molecules and form a stable complex with pesticides, thus promoting the adsorption of pesticides in soil (Khalid *et al.* 2020). In addition, the loose and porous surface structure of soil OM provides

more adsorption sites for DEA molecules and promotes the fixation of DEA in soil. The DEA adsorption reaction of soil is predominantly based on the protonated carboxyl group and molecular state (Huang and Weber 1997). Furthermore, the adsorption capacity of soil colloids for the protonated carboxyl group is enhanced with increased soil CEC, which improves the DEA adsorption capacity of the three types of soil.

The $1/n$ values of the Freundlich model can be used to describe the nonlinear degree of adsorption isotherm, thereby revealing the DEA adsorption mechanism by pristine and BC soil. The values of $1/n < 1$ indicate “L-shaped” adsorption isotherms, whereas $1/n > 1$ suggests “S-shaped” adsorption isotherms. When $1/n = 1$, the adsorption isotherms were consistent with the linear adsorption model. According to Table 2, the DEA adsorption fitting parameter of $1/n$ of all soils were 0.494 to 0.982, indicating an “L-type” adsorption isotherm. This indicated that the adsorption process of all soils consisted of two mechanisms: linear partitioning and nonlinear surface adsorption. The nonlinear degree of the adsorption isotherm increased as $1/n$ decreased. The Freundlich parameter of $1/n$ for the three BC soils for DEA were lower than those of the pristine soils, which indicated that the nonlinearity of the DEA adsorption isotherm was enhanced by the addition of biochar. The Freundlich $1/n$ values of the three pristine soils for DEA were 0.791 to 0.982, indicating approximately linear adsorption isotherms. The $1/n$ value can also describe the adsorption intensity of the adsorbent, *i.e.*, the adsorption intensity decreases with increasing $1/n$ value. When $1/n > 1$, the adsorption process is relatively unreactive (Wang *et al.* 2019). Thus, in this study, the DEA adsorption intensity was greater for the three BC soils than the three pristine soils.

Effects of Biochar on DEA Adsorption Thermodynamics

The thermodynamic analysis of the adsorption process was performed to investigate the disorder degree of the adsorption reaction system and the motivating factors on which the adsorption reaction relied. The thermodynamic parameters of DEA adsorption on the three soils and BC soils at 15 °C, 25 °C, and 35 °C are shown in Table 3. The ΔG ($\text{kJ}\cdot\text{mol}^{-1}$) value denotes the change of Gibbs free energy, which is an important parameter for investigating the energy changes of adsorption reactions (Asadullah *et al.* 2019). The ΔG value reflects the relative favorability of the adsorption reaction; the more negative the value of ΔG , the more thorough the reaction. As shown in Table 3, the ΔG value of the adsorption process of the three pristine soils for DEA was greater than that of the BC soils. This demonstrated that the adsorption of three pristine soils for DEA was less favorable and the adsorption amount was smaller. This was validated by the experimental results. The equilibrium adsorption amount of red soil, brown soil, and black soil for DEA merely accounted for 3.4%-4.7%, 0.9%-7.2%, and 10.1%-12.7% of the initial DEA addition at 15 °C, respectively. The equilibrium adsorption amount of red soil, brown soil, and black soil for DEA accounted for 1.8%-2.6%, 3%-4.9%, and 6.7%-10.9% of the initial DEA addition at 25 °C, respectively. The adsorption percentages of red soil, brown soil, and black soil were 1.5%-2.7%, 1.7%-6.9%, and 7.2%-12.8% at 35 °C, respectively. Similar behavior was observed by Srivastava *et al.* (2006), Ramadhani *et al.* (2020), Siyal *et al.* (2020), Niero *et al.* (2020), and Tam *et al.* (2020). This was possibly related to physical adsorption associated with diffusion phenomenon and ionic interactions (Khan *et al.* 2020).

The DEA molecule contains $-\text{NH}_2$, $-\text{Cl}$, and $-\text{NH}$ groups. The $-\text{Cl}$ group on the benzene ring has an electrophilic and electronegative character. Similarly, the $-\text{NH}_2$ was active and was easily oxidized to $-\text{NO}_2$, which has stronger electrophile capability than

adjacent carbon atom on the benzene ring. The electron density on the benzene ring is shifted towards the $-NO_2$ group, due to its electronegativity. The electronegative $-NO_2$ and $-Cl$ groups in DEA molecule repelled the negative charges in the three pristine soils colloid. This may have led to the formation of an energy barrier which restrained the adsorption of three pristine soils for DEA (Araujo *et al.* 2018). However, the N atom of $-NH_2$ has a lone pair electron and presented p- π conjugation with electron cloud on the benzene ring. The $-NH_2$ played a dominant role of electron-donor. Therefore, the electropositive $-NH_2$ group was attracted to negative charges in the soil colloid. Hence, in the premise of short experiment duration without complete transformation of $-NH_2$ to $-NO_2$, the electropositive $-NH_2$ may overcome the energy barrier, and a small amount of DEA may be adsorbed by the three pristine soils. The ΔG values of DEA adsorption for the three BC soils increased with decreasing temperature: $\Delta G_{35\text{ }^\circ\text{C}} < \Delta G_{25\text{ }^\circ\text{C}} < \Delta G_{15\text{ }^\circ\text{C}}$. This indicated that a higher temperature was more conducive to the DEA adsorption process in BC soil and enabled more thorough adsorption (at 35 °C). Therefore, the DEA adsorption process in the three BC soils was an endothermic reaction, requiring a large amount of energy to transfer DEA from the water phase to the solid phase.

Table 3. DEA Adsorption Thermodynamic Parameters in Three Pristine Soils and BC Soils

Temperature	ΔG (kJ·mol ⁻¹)			ΔH	ΔS
	15 °C	25 °C	35 °C		
Red Soil	4.092	5.101	5.503	-16.318	-0.071
Brown Soil	2.476	3.125	8.077	-77.453	-0.275
Black Soil	0.349	0.020	1.299	-23.933	-0.081
BC Red Soil	-5.739	-6.356	-7.060	13.275	0.066
BC Brown Soil	-4.284	-5.447	-5.857	18.499	0.080
BC Black Soil	-4.203	-5.047	-5.487	14.352	0.065

The ΔS value reflects the change of entropy in a reaction system. Thus, $\Delta S > 0$ indicates a process where entropy is increasing, and the internal disorder degree of the system increases. Conversely, $\Delta S < 0$ describes a process where entropy is decreasing, and the disorder degree of the reaction system decreases. According to Table 3, the ΔS values of the DEA adsorption process for pristine soil were negative, which indicates that entropy was reduced in the course of adsorption; the DEA adsorption reduced the degree of freedom of the system, and the adsorption reaction was an associative process (Tran *et al.* 2016). The ΔS values of the DEA adsorption process of the three BC soils were positive, indicating that entropy was increasing, and the DEA adsorption process increased the energy and degree of freedom of the reaction system. In addition, the disorder degree of the solid-liquid interface increased, reflecting the enhanced adsorption affinity of the three BC soils for DEA (Yao *et al.* 2014).

The ΔH value indicates the enthalpy change of a system, which reveals the energy change of a system (Asadullah *et al.* 2019). Thus, $\Delta H > 0$ indicates that the adsorption process is an endothermic process and that increased temperature is conducive to the adsorption. Conversely, $\Delta H < 0$ indicates an exothermic process, that typically is favored by a relatively low temperature. The ΔH values of the DEA adsorption process for the three pristine soils were negative, which indicate an exothermic interaction (Table 3).

Conversely, the ΔH values of DEA adsorption for BC soil were positive, which indicated that the adsorption process became an endothermic reaction after the addition of tall fescue biochar. Adsorption was a physicochemical process that retained pesticide molecules on the surface of the solid by hydrophobic interaction, hydrogen bonding, ionic bonding, and Van der Waals force mechanisms. The absolute value of ΔH was used to evaluate the force on which the reaction relied. For example, ΔH values of 4 to 10 indicate Van der Waals forces, ΔH values of approximately 5 indicate hydrophobic interaction, ΔH values of 2 to 40 indicate the formation of hydrogen bonds, ΔH values of approximately 40 indicate ion-exchange, ΔH values of 2 to 29 indicate dipole bond forces, and ΔH values > 60 indicate the formation of chemical bonds (Von Oepen *et al.* 1991). Therefore, the results indicate that DEA adsorption for three pristine soils and BC soils predominantly relied on the formation of hydrogen bonds (ΔH 2 to 40 $\text{kJ}\cdot\text{mol}^{-1}$) and the dipole bond force (ΔH 2 to 29 $\text{kJ}\cdot\text{mol}^{-1}$), with chemical bonding also involved in the DEA adsorption process of pristine brown soil ($\Delta H > 60 \text{ kJ}\cdot\text{mol}^{-1}$).

DEA Adsorption Mechanism for the Three Soils and BC Soils

Due to the heterogeneity of soil and biochar surfaces, a single adsorption mechanism cannot completely describe the adsorption process of soil and biochar for organic pollutants. Chiou *et al.* (2015) suggested that the adsorption mechanism of biochar for organic pollutants was predominantly partitioning and surface adsorption. Biochars do not undergo complete carbonization, and they typically contain two structures. The carbonized content of biochars exhibits as glassy surface, while the noncarbonized fraction has a rubbery surface. Contaminant adsorption on the glassy surface can be attributed to surface adsorption, whereas the adsorption of contaminant molecule in a rubbery surface is mainly dependent on partitioning phenomena (Zheng *et al.* 2010). Partitioning refers to the dissolution of organic adsorbate by organic components of adsorbent. The partitioning mechanism is closely related to the solubility of the organic adsorbate rather than adsorption site.

The isothermal adsorption curve of partitioning was linear and non-competitive, whereas surface adsorption was nonlinear and competitive. The partitioning was illustrated by the approximate linear isotherm and independent uptakes by the amorphous organic phase of adsorbent (Chiou *et al.* 1985). However, in this study, the contribution of partitioning and surface adsorption to the total adsorption amount differed for the three soils and BC soils. A quantitative analysis of their relative contribution to the total adsorption capacity is shown in Fig. 5 (a through f), where (a), (c), and (e) represent the relative contributions of surface adsorption and partitioning for the three pristine soils, and (b), (d), and (f) represent the same for BC red soil, BC brown soil, and BC black soil, respectively. The contribution of partitioning for the three pristine soils was clearly greater than that of surface adsorption and close to the total adsorption amount (93.7%, 88.0%, and 64.6% for red soil, brown soil, and black soil, respectively). This may be because of the lack of adsorption sites on the surface of soil particles. The DEA in a low-porosity solution-soil system may be adsorbed more effectively by a non-competitive partition process than by a competitive surface adsorption process. Conversely, at relatively low equilibrium concentrations, the contribution of surface adsorption was greater than that of partitioning for BC soil; however, as the equilibrium solution concentration increased, the contribution of partitioning gradually exceeded that of surface adsorption. This may be because of the relatively high affinity between DEA molecules and tall fescue biochar at relatively low equilibrium concentrations, which increased surface adsorption sharply.

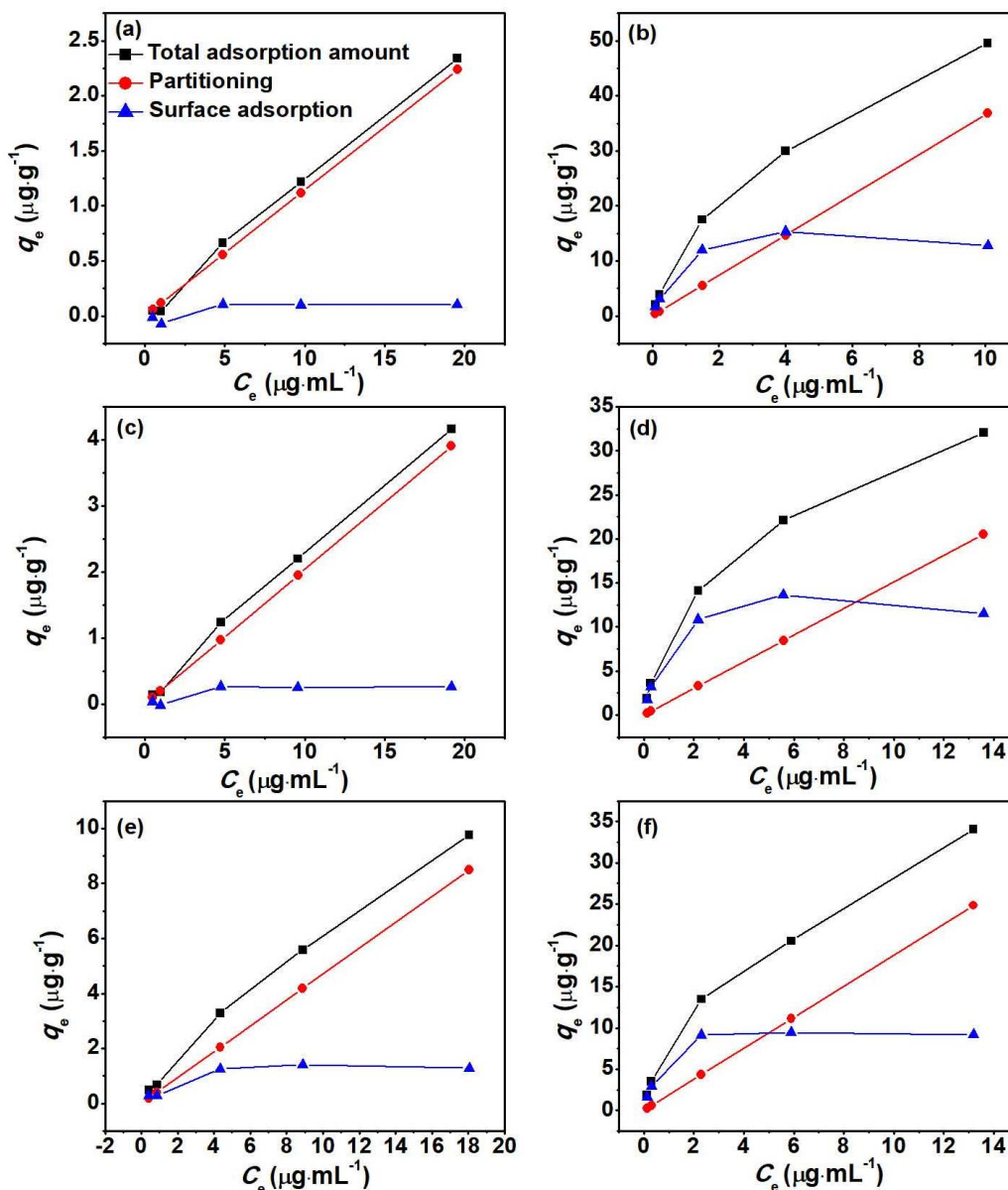


Fig. 5. Contribution of partitioning and surface adsorption to the total DEA adsorption amount for three pristine soils and BC soils: (a) red soil; (b) BC red soil; (c) brown soil; (d) BC brown soil; (e) black soil; and (f) BC black soil

At this time, DEA molecules were adsorbed on the surface of soil minerals and biochar crystal components by physicochemical adsorption. The tall fescue was transformed into a glassy material with a dense structure after pyrolyzing, resulting in an uneven porous structure, relatively dense adsorption domains, high-energy adsorption sites, a developed pore structure, and a large specific surface area. The addition of biochar increased the active adsorption sites of the soil surface, enabling DEA to rapidly bind to the adsorption sites on the biochar surface. The heterocyclic structure of DEA was the electron donor, which had an electron donor–receptor reaction (EDA) with the electron acceptor of the biochar, thereby promoting the surface adsorption of DEA by the biochar-soil system. In addition, DEA can also act as a hydrogen bond donor and acceptor to form

hydrogen bonds with H, N, or O on the surface of biochar, thus improving its adsorption affinity on the surface of the biochar (Wang *et al.* 2019). With increased DEA equilibrium concentration, the adsorption sites on the surface of the tall fescue biochar were gradually occupied. Thus, DEA molecules were partitioned to the soil OM and amorphous components of biochar. This is consistent with the results of Zhang *et al.* (2018b), whereby the adsorption of pesticides at relatively low equilibrium concentrations was controlled by the high-energy adsorption sites of biochar. Conversely, the partial adsorption sites of the carbonized OM of biochar were saturated, enabling hydrophobic partitioning to become the dominant process.

CONCLUSIONS

1. The addition of biochar remarkably improved the desethyl-atrazine (DEA) adsorption capacity of red soil, brown soil, and black soil, with the greatest improvement for red soil, which has relatively low organic matter (OM).
2. The pseudo-second-order equation most closely fitted the adsorption kinetics. Both the Freundlich and Langmuir isotherms fit well to the equilibrium adsorption data for the soils. Equilibrium DEA adsorption increased with increasing equilibrium concentration.
3. The DEA adsorption process in the three pristine soils was exothermic and less thorough; then it became an endothermic and more thorough reaction after the addition of biochar.
4. The partitioning mechanism was dominant in the DEA adsorption process for pristine soil, whereas surface adsorption was dominant in the biochar treatment group (BC) soil at a relatively low equilibrium concentration. As the equilibrium concentration increased, the contribution of partitioning exceeded that of surface adsorption in BC soil.
5. All the mentioned results corroborate the effectiveness of tall fescue biochar in the reduction of DEA from polluted soil and reveal the dominating mechanism. Therefore, these findings have important applications for the future remediation of DEA from the environment using tall fescue biochar material. However, the different pesticide metabolites exhibited various properties. Research on different types of metabolites should be strengthened in the future.

ACKNOWLEDGEMENTS

This study was supported by the National Natural Science Foundation of China (grant numbers 41501542 and 41471389).

REFERENCES CITED

- Aguilar, J. A. P., Andreu, V., Campo, J., Pico, Y., and Masia, A. (2017). "Pesticide occurrence in the waters of Júcar River, Spain from different farming landscapes," *Sci. Total Environ.* 607-608, 752-760. DOI: 10.1016/j.scitotenv.2017.06.176

- Ahmed, S. M., Taha, M. R., and Taha, O. M. E. (2018). "Kinetics and isotherms of dichlorodiphenyltrichloroethane (DDT) adsorption using soil-zeolite mixture," *Nanotechnology for Environmental Engineering* 3, Article number 4. DOI: 10.1007/s41204-017-0033-8
- Aljeboree, A. M., Alkaim, A. F., and Al-Dujaili, A. H. (2015). "Adsorption isotherm, kinetic modeling and thermodynamics of crystal violet dye on coconut husk-based activated carbon," *Desalin. Water Treat.* 53(13), 3656-3667. DOI: 10.1080/19443994.2013.877854
- Araujo, L. A., Bezerra, C. O., Cusioli, L. F., Silva, M. F., Nishi, L., Gomes, R. G., Bergamasco, R. (2018). "Moringa oleifera biomass residue for the removal of pharmaceuticals from water," *J. Environ. Chem. Eng.* 6, 7192-7199. DOI: 10.1016/j.jece.2018.11.016
- Asadullah, Lupong, K., and Kanogwan, T. (2019). "Adsorption of hexavalent chromium onto alkali-modified biochar derived from *Lepironia articulata*: A kinetic, equilibrium, and thermodynamic study," *Water Environ. Res.* 91(11), 1433-1446. DOI: 10.1002/wer.1138
- Binh, Q. A., and Kajitvichyanukul, P. (2019). "Adsorption mechanism of dichlorvos onto coconut fibre biochar: The significant dependence of H-bonding and the pore-filling mechanism," *Water Sci. Technol.* 79(5), 866-876. DOI: 10.2166/wst.2018.529
- Bogusz, A., Oleszczuk, P., and Dobrowolski, R. (2017). "Adsorption and desorption of heavy metals by the sewage sludge and biochar-amended soil," *Environ. Geochem. Health* 41(4), 1663-1674. DOI: 10.1007/s10653-017-0036-1
- Braida, W. J., Pignatello, J. J., Lu, Y. F., Ravikovitch, P. I., Neimark, A. V., and Xing, B. S. (2003). "Sorption hysteresis of benzene in charcoal particles," *Environ. Sci. Technol.* 37(2), 409-417. DOI: 10.1021/es020660z
- Chen, Y., Shan, R. F., and Sun, X. Y. (2020). "Adsorption of cadmium by magnesium-modified BC at different pyrolysis temperatures," *BioResources* 15(1), 767-786. DOI: 10.15376/biores.15.1.767-786
- Chiou, C. T., Cheng, J. Z., Hung, W., Chen, B. L., and Lin T. (2015). "Resolution of adsorption and partition components of organic compounds on black carbons," *Environ. Sci. Technol.* 49(15), 9116-9123. DOI: 10.1021/acs.est.5b01292
- Chiou, C. T., Shoup, T. D., Porter, P. E. (1985). "Mechanistic roles of soil humus and minerals in the sorption of nonionic organic compounds from aqueous and organic solutions," *Org. Geochem.* 8, 9-14. DOI: 10.1016/0146-6380(85)90045-2
- Ding, T. D., Huang, T., Wu, Z. H., Li, W., Guo, K. X., and Li, J. Y. (2019). "Adsorption-desorption behavior of carbendazim by sewage sludge-derived biochar and its possible mechanism," *RSC Adv.* 9(60), 35209-35216. DOI: 10.1039/c9ra07263b
- European Commission (2009). "EU pesticides database," European Commission, (<http://ec.europa.eu/food/plant/pesticides/eu-pesticides-database/public/?event=homepage&language=ENhttp>), Accessed 17 March 2009.
- Grung, M., Lin, Y., Zhang, H., Steen, A. O., Huang, J., Zhang, G., and Larssen, T. (2015). "Pesticide levels and environmental risk in aquatic environments in China--A review," *Environmental International* 81, 87-97. DOI: 10.1016/j.envint.2015.04.013
- Guo, J. H., Li, Z. N., Ranasinghe, P., Bonina, S., Hosseini, S., Corcoran, M. B., Smalley, C., Kaliappan, R., Wu, Y., Chen, D., *et al.* (2016). "Occurrence of atrazine and related compounds in sediments of upper great lakes," *Environ. Sci. Technol.* 50(14), 7335-7343. DOI: 10.1021/acs.est.6b00706

- Hall, K. E., Ray, C., Ki, S. J., Spokas, K. A., and Koskinen, W. C. (2015). "Pesticide sorption and leaching potential on three Hawaiian soils," *J. Environ. Manage.* 159, 227-234. DOI: 10.1016/j.jenvman.2015.04.046
- Ho, Y. S. (2006). "Review of second-order models for adsorption systems," *J. Hazard. Mater.* 136(3), 681-689. DOI: 10.1016/j.jhazmat.2005.12.043
- Huang, W. L., and Weber, W. J. (1997). "A distributed reactivity model for sorption by soils and sediments. 10. Relationship between desorption, hysteresis, and the chemical characteristics of organic domains," *Environ. Sci. Technol.* 31(9), 2562-2569. DOI: 10.1021/es960995e
- Hubbe, M. A., Azizian, S., and Douven, S. (2019). "Implications of apparent pseudo-second-order adsorption kinetics onto cellulosic materials: A review," *BioResources* 14(3), 7582-7626. DOI: 10.15376/biores.14.3.7582-7626
- Kerminen, K., Salovaara, V., and Kontro, M. H. (2017). "A zero-valent iron and organic matter mixture enhances herbicide and herbicide degradation product removal in subsurface waters," *J. Environ. Sci.* 57, 411-417. DOI: 10.1016/j.jes.2016.12.013
- Khalid, S., Shahid, M., Murtaza, B., Bibi, I., Natasha, Naeem, M. A., and Niazi, N. K. (2020). "A critical review of different factors governing the fate of pesticides in soil under biochar application," *Sci. Total Environ.* 711, Article ID 134645. DOI: 10.1016/j.scitotenv.2019.134645
- Khan, H., Iram, Gul, K., Ara, B., Khan, A., Ali, N., Ali, N., and Bilal, M. (2020). "Adsorptive removal of acrylic acid from the aqueous environment using raw and chemically modified alumina: Batch adsorption, kinetic, equilibrium and thermodynamic studies," *J. Environ. Chem. Eng.* DOI: 10.1016/j.jece.2020.103927
- Kolpin, D. W., Thurman, E. M., and Linhart, S. M. (2000). "Finding minimal herbicide concentrations in ground water? Try looking for their degradates," *Sci. Total Environ.* 248(2-3), 115-122. DOI: 10.1016/S0048-9697(99)00535-5
- Komtchou, S., Delegan, N., Dirany, A., Drogui, P., Robert, D., and Khakani, M. A. (2018). "Removal of atrazine by photoelectrocatalytic process under sunlight using WN-codoped TiO₂ photoanode," *J. Appl. Electrochem.* 48, 1353-1361. DOI: 10.1007/s10800-018-1253-8
- Kumar, A., and Singh, N. (2016). "Atrazine and its metabolites degradation in mineral salts medium and soil using an enrichment culture," *Environ. Monit. Assess.* 188(3), Article number 142. DOI: 10.1007/s10661-016-5144-3
- Li, W. T., Shan, R. F., Fan, Y. N., and Sun, X. Y. (2020). "Effects of tall fescue biochar on the adsorption and desorption of atrazine in different types of soil," *Environ. Sci. Pollut. R.* (Online). DOI: 10.1007/s11356-020-10821-0
- Masia, A., Ibanez, C., Blasco, C., Sancho, J. V., Pico, Y., and Hernandez, F. (2013). "Combined use of liquid chromatography triple quadrupole mass spectrometry and liquid chromatography quadrupole time-of-flight mass spectrometry in systematic screening of pesticides and other contaminants in water samples," *Anal. Chim. Acta* 761, 117-127. DOI: 10.1016/j.aca.2012.11.032
- Montiel-Leon, J. M., Duy, S. V., Munoz, G., Bouchard, M. F., Amyot, M., and Sauve, S. (2019a). "Quality survey and spatiotemporal variations of atrazine and desethylatrazine in drinking water in Quebec, Canada," *Sci. Total Environ.* 671, 578-585. DOI: 10.1016/j.scitotenv.2019.03.228
- Montiel-Leon, J. M., Munoz, G., Von, D. S., Do, D. T., Vaudreuil, M., Goeury, K., Guillemette, F., Amyot, M., and Sauve, S. (2019b). "Widespread occurrence and spatial distribution of glyphosate, atrazine, and neonicotinoids pesticides in the St.

- Lawrence and tributary rivers,” *Environ. Pollut.* 250, 29-39. DOI: 10.1016/j.envpol.2019.03.125
- Niero, G., Rodrigues, C. A., Almerindo, G. I., Correa, A. X. R., Gaspareto, P., Feuzer-Matos, A. J., Somensi, C. A., and Radetski, C. M. (2020). “Using basic parameters to evaluate adsorption potential of alternative materials: example of amoxicillin adsorption by activated carbon produced from termite bio-waste,” *J. Environ. Sci. Health Part A*. DOI: 10.1080/10934529.2020.1835125
- Okoya, A. A., Adegaju, O. S., Akinola, O. E., Akinyele, A. B., and Amuda, O. S. (2020). “Comparative assessment of the efficiency of rice husk biochar and conventional water treatment method to remove from pesticide polluted water,” *Current Journal of Applied Science and Technology* 39(2), 1-11. DOI: 10.9734/cjast/2020/v39i230491
- Pholosi, A., Naidoo, E. B., Ofomaja, A. E. (2020). “Intraparticle diffusion of Cr(VI) through biomass and magnetite coated biomass: A comparative kinetic and diffusion study,” *South African Journal of Chemical Engineering* 32, 39-55. DOI: 10.1016/j.sajce.2020.01.005
- Qiu, Y., Xiao, X., Cheng, H., Zhou, Z., and Sheng, G. D. (2009). “Influence of environmental factors on pesticide adsorption by black carbon: pH and model dissolved organic matter,” *Environ. Sci. Technol.* 43(13), 4973-4978. DOI: 10.1021/es900573d
- Ramadhani, P., Chaidir, Z., Zilfa., Tomi, Z. B., Rahmiarti, D., and Zein, R. (2020). “Shrimp shell (*Metapenaeus monoceros*) waste as a low-cost adsorbent for metanil yellow dye removal in aqueous solution,” *Desalin. Water Treat.* 197, 413-423. DOI: 10.5004/dwt.2020.25963
- Sánchez, V., Lopez-Bellido, F. J., Rodrig, M. A., Fernandez, F. J., and Rodriguez, L. (2020). “A mesocosm study of electrokinetic-assisted phytoremediation of atrazine-polluted soils,” *Sep. Purif. Technol.* 233, Article ID 116044. DOI: 10.1016/j.seppur.2019.116044
- Siyal, A. A., Shamsuddin, R., Low, A., Hidayat, A. (2020). “Adsorption kinetics, isotherms, and thermodynamics of removal of anionic surfactant from aqueous solution using fly ash,” *Water. Air. Soil. Pollut.* 231, 327-332. DOI: 10.1007/s11270-020-04879-2
- Srivastava, V. C., Swamy, M. M., Mall, I. D., Prasad, B., Mishra, I. M. (2006). “Adsorptive removal of phenol by bagasse fly ash and activated carbon: Equilibrium, kinetics and thermodynamics,” *Colloid Surf. A-Physicochem. Eng. Asp.* 272, 89-104. DOI: 10.1016/j.colsurfa.2005.07.016
- Sun, X. Y., Shan, R. F., Li, X. H., Pan, J. H., Liu, X., Deng, R. N., and Song, J. Y. (2017). “Characterization of 60 types of Chinese biomass waste and resultant biochars in terms of their candidacy for soil application,” *Glob. Change Biol. Bioenergy* 9(9), 1423-1435. DOI: 10.1111/gcbb.12435
- Tam, N. T. M., Liu, Y. G., and Thom, N. V. (2020). “Magnetic gelatin-activated biochar synthesis from agricultural biomass for the removal of sodium diclofenac from aqueous solution: adsorption performance and external influence,” *Int. J. Environ. Anal. Chem.* DOI: 10.1080/03067319.2020.1832483
- Tran, H. N., You, S. J., and Chao, H. P. (2016). “Thermodynamic parameters of cadmium adsorption onto orange peel calculated from various methods: A comparison study,” *Journal of Environmental Chemical Engineering* 4(3), 2671-2682. DOI: 10.1016/j.jece.2016.05.009

- Uwamungu, J. Y., Nartey, O. D., Uwimpaye, F., Dong, W. X., and Hu, C. S. (2019). "Evaluating biochar impact on topsoil adsorption behavior on soil under no-tillage and rotary tillage treatments: Isotherms and kinetics," *Int. J. Env. Res. Pub. He.* 16(24), Article number 5034. DOI: 10.3390/ijerph16245034
- Von Oepen, B., Kordel, W., and Klein, W. (1991). "Sorption of nonpolar and polar compounds to soils: Processes, measurements and experience with the applicability of the modified OECD-Guideline 106," *Chemosphere* 22(3-4), 285-304. DOI: 10.1016/0045-6535(91)90318-8
- Wang, J. X., and Zhang, W. J. (2021). "Evaluating the adsorption of Shanghai silty clay to Cd(II), Pb(II), As(V), and Cr(VI): kinetic, equilibrium, and thermodynamic studies," *Environ. Monit. Assess.* 193, 131. DOI: 10.1016/J.SAJCE.2020.01.005
- Wang, J. Y., Zhang, M., Xiong, Z. Q., Liu, P. L., and Pan, G. X. (2011). "Effects of biochar addition on N₂O and CO₂ emissions from two paddy soils," *Biol. Fert. Soils* 47, 887-896. DOI: 10.1007/s00374-011-0595-8
- Wang, P. P., Liu, X. G., Yu, B. C., Wu, X. H., Dong, F. S., and Zheng, Y. Q. (2019). "Characterization of peanut-shell biochar and the mechanisms underlying its sorption for atrazine and nicosulfuron in aqueous solution," *Sci. Total Environ.* 702, Article ID 134767. DOI: 10.1016/j.scitotenv.2019.134767
- Wei, L., Huang, Y. F., Li, Y. L., Huang, L. X., Mar, N. N., Huang, Q., and Liu, Z. Z. (2017). "Biochar characteristics produced from rice husks and their sorption properties for the acetanilide herbicide metolachlor," *Environ. Sci. Pollut. R.* 24, 4552-4561. DOI: 10.1007/s11356-016-8192-x
- Yao, Q. X., Xie, J. J., Liu, J. X., Kang, H. M., and Liu, Y. (2014). "Adsorption of lead ions using a modified lignin hydrogel," *J. Polym. Res.* 21, Article no. 465. DOI: 10.1007/s10965-014-0465-9
- Yu, J., Bian, Z. Q., Tian, X. H., Zhang, J., Zhang, R., and Zheng, H. H. (2018). "Atrazine and its metabolites in surface and well waters in rural area and its human and ecotoxicological risk assessment of Henan province, China," *Hum. Ecol. Risk Assess.* 24(1), 1-13. DOI: 10.1080/10807039.2017.1311768
- Zhang, P., Ren, C., Sun, H. W., and Min, L. J. (2018a). "Sorption, desorption and degradation of neonicotinoids in four agricultural soils and their effects on soil microorganisms," *Sci. Total Environ.* 615, 59-69. DOI: 10.1016/j.scitotenv.2017.09.097
- Zhang, P., Sun, H. W., Ren, C., Min, L. J., and Zhang, H. M. (2018b). "Sorption mechanisms of neonicotinoids on biochars and the impact of deashing treatments on biochar structure and neonicotinoids sorption," *Environ. Pollut.* 234, 812-820. DOI: 10.1016/j.envpol.2017.12.013
- Zhang, P., Sun, H. W., Yu, L., and Sun, T. H. (2013). "Adsorption and catalytic hydrolysis of carbaryl and atrazine on pig manure — derived biochars: Impact of structural properties of biochars," *J. Hazard. Mater.* 244-245, 217-224. DOI: 10.1016/j.jhazmat.2012.11.046
- Zhang, Y., Li, W., Zhou, W. W., Jia, H. R., and Li, B. T. (2020). "Adsorption-desorption characteristics of pyraclonil in eight agricultural soils," *J. Soil. Sediment.* 20, 1404-1412. DOI: 10.1007/s11368-019-02471-8
- Zhao, Z. D., Wu, Q. Q., Nie, T. T., and Zhou, W. J. (2019). "Quantitative evaluation of relationships between adsorption and partition of atrazine in biochar-amended soils with biochar characteristics," *RSC Adv.* 9(8), 4162-4171. DOI: 10.1039/C8RA08544G

Zheng, W., Guo, M., Chow, T., Bennett, D. N., and Rajagopalan, N. (2010). "Sorption properties of green waste biochar for two triazine pesticides," *J. Hazard. Mater.* 181, 121-126. DOI: 10.1016/j.jhazmat.2010.04.103

Article submitted: October 27, 2020; Peer review completed: February 21, 2021; Revised version received: March 19, 2021; Accepted: March 24, 2021; Published: March 29, 2021.

DOI: 10.15376/biores.16.2.3575-3595